Simulation and Control of Linear Fresnel Reflector Solar Plant

Rowida Meligy*, Mohamed Rady**, Adel El Samahy***, Waeel Mohamed***, Filippo Paredes****, Fabio Montagnino ****

* Mechanical Engineering Department, Helwan University, Helwan, Egypt

** Mechanical Engineering Department, Faculty of Engineering, King Abdulaziz University, Rabigh Campus, Saudi Arabia
Faculty of Engineering, Helwan University, Egypt

***Electrical Engineering Department, Helwan University, Helwan, Egypt

****Consorzio ARCA - Solar Living Lab, Viale delle Scienze Building 16, 90128 Palermo, Italy

(rowida.meligy@h-eng.helwan.edu.eg, maradhi@kau.edu.sa, El_Samahya@yahoo.com, canadawy@hotmail.com, fparedes@consorzioarca.it, fmontagnino@consorzioarca.it)

‡ Rowida Meligy, Helwan University, Helwan-11795, Egypt,

rowida.meligy@h-eng.helwan.edu.eg

Received: 04.03.2019 Accepted:14.04.2019

Abstract - Linear Fresnel Reflector (LFR) solar collectors is a promising technology that has a good potential for small scale solar applications such as heating, cooling and power generation. The present article presents simulation and control study of a small-scale multi-generation LFR solar power plant located in SEKEM medical center near Belbis city, Egypt. In this study Conventional and Renewable Energy Optimization Toolbox (CARNOT) has been adopted for the first time to model the LFR solar field. A quasi-dynamic model of LFR has been implemented in the environment of MATLAB/Simulink, which includes LFR collector, storage tank, pipes and centrifugal pump. The LFR model has been successfully validated using experimental data obtained from LFR solar collector in the test field of the Solar Living Lab of Consorzio ARCA in Palermo, Italy. Proportional Integral (PI) plus feed forward controller (both parallel and series configurations) with an anti-reset mechanism have been developed. The controller has been applied to maintain the difference between the outlet and inlet temperature of LFR collector at a constant value under different conditions of disturbances due to variation of ambient temperature, inlet oil temperature and solar radiation. The performance of the controllers have been evaluated under nominal conditions, presence of disturbance, and change in operating conditions.

Keywords- Solar power technologies; Linear Fresnel Reflector; Temperature control; CARNOT toolbox; Feed forward control; PI controller.

Nomenclature

A_{loss}	Surface area for losses	(m²)
A_{net}	Net area of mirror surface	(m²)
a_0	Pump constant coefficient	(pa)
a_1	Pump linear coefficient	(Pa .s/kg)
a_2	Pump quadratic coefficient	(Pa. (s /kg)^2)
b_0	Pressure drop constant coefficient	(pa)
b_1	Pressure drop linear coefficient	(Pa .s/kg)
b_2	Pressure drop quadratic coefficient	(Pa. (s /kg)^2)
C	Heat capacity of fluid	(J/kg .K)
C_{col}	Heat capacity of collector per unit surface area	(J/(m².K)
C_{wall}	Heat capacity of pipe wall per unit length	(J/(m K))
Δz	Distance between two nodes	(m)
K_P	Controller proportional gain	(-)
$L_{reciever}$	Length of the receiver tube	(m)

$\dot{m}$	Mass flow rate	(kg/s)
$\dot{Q}_{useful}$	Useful thermal energy produced by the solar field	(W)
$\dot{Q}_{abs}$	Thermal energy absorbed by the solar receiver	(W)
$\dot{Q}_{loss}$	Thermal energy lost from the absorber pipe	(W)
$\dot{q}_{solar}$	Solar radiation power input per surface area	(W/m²)
T_{amb}	Ambient temperature	(K)
T_{sky}	Sky temperature	(K)
T_i	Integration time	(s)
T_m	Average collector temperature	(K)
U	Heat loss coefficienct	(W/(m²K))
U_{wind}	Wind speed dependence of the heat loss coefficient	(J/(m³K))
U_{sky}	Sky temperature dependence of the heat loss coefficient	(W/(m²K))
U_1	Linear heat loss coefficient	(W/(m²K))
U_2	Quadratic heat loss coefficient	(W/(mK)²)
V_{node}	Node volume	(m^3)
V_{wind}	Mean wind speed	(m/s)
X	Mean distance between primary mirrors and the receiver	(m)
ρ	Fluid density	(kg/m^3)
Δh	Input-output specific energy gradient	(J/kg)
λ_{eff}	effective axial thermal conductivity	(W/mK)

Subscripts

Col	Collector
eff	Effective
abs	Absorbed
amb	Ambient
Node	Calculation node

1. Introduction

Energy from the solar radiation has the largest potential for providing abundant, clean, safe, and reliable power. The Concentrated Solar Power (CSP) systems are employed to reflect and concentrate sunlight onto receivers that collect solar energy and convert it into heat. This thermal power can be converted into electricity via a steam turbine or a heat engine driving a generator. There are four main categories of CSP technologies classified according to the distribution of the focused solar radiation on the receiver into linear and punctual focus technologies [1]. According to the sun tracking mechanisms, CSP can be classified into single and two axes tracking technologies [2]. Central Tower Receivers (CTR) and Parabolic Dish Collectors (PDC) employ two-axis tracking systems and punctual focus technologies. The Parabolic Trough Collectors (PTC) and the Linear Fresnel Reflector (LFR) employ single axis tracking and linear focus technologies.

LFR is recently entering into the market with small scale projects. It is composed of many long rows segments of shallow curvature or flat mirrors. The mirrors focus the sunlight onto a fixed elevated tubular receiver running parallel to the reflector rotational axis. Mirror segments are aligned horizontally and track the sun such that the receiver is illuminated without the need for being moved. A secondary reflector can be installed on top of the receiver tube to enhance the captured sunlight [3]. The operating temperature of LFR is usually between 250 and 500°C [4], even if lower temperature setting may be implemented, in agreement with the specific application.

Linear Fresnel reflector appears to be the main competitor to PTC with advantages of reducing the installation costs as due to lighter structures [5]. In addition to, having simpler tracking systems, less land occupation and less resistance to the wind. However, LFR has a relatively lower optical quality and thermal efficiencies compared to parabolic trough collector [6].

CSP plants are usually developed in a large-scale, however, in the recent years, an attractive option of applying those in multi-generation at a small and micro scale is emerging as an alternative for powering remote, rural and off-grid applications [42] [42].

Design and optimization of the operation of small-scale multi-generation solar plant requires the development of a robust simulation, control and energy management system. Efficient energy management system is a fundamental task that must be embedded with the ability to reduce costs for end consumers, maximization of power production, minimization of energy losses and avoiding possible overload or blackout [9-11]. This is usually done taking into account the predicted price of electricity, forecasting of load, predicted solar radiation and other factors.

In a recent EU-funded project, Small scale Thermal Solar districts for Mediterranean communities (STS-MED), a solar multi-generation approach has been implemented in four different countries (Cyprus, Egypt, Jordan, Italy), each characterized by different collectors and different integration scenarios [12].

In Egypt, the STS-MED plant, including LFR collectors (model IDEA 1FC-1832), has been installed at the SEKEM medical center near the Belbis city (Lat. 30°25'05.5"N, Long. 31°38'07.8"E, atlitude 35m). Another plant, including the same LFR collector model, has been commissioned in Palermo, Italy (Lat. 38°06'01.0"N, Long. 13°20'37.3"E, altitude 50m).Finally, a third LFR IFC-1832 collector has been installed in Nicosia, Cyprus (Lat. 35°08'28.1"N , Long. 33°22'50.7"E, elevation 176m).The work presented here is the first part of an ongoing joint research on modeling and hierarchical control architecture of multi-generation solar plants, which is leveraging this network of demonstrative systems.

2. Literature Survey

This section is devoted to the analsyis and discussion of the previous related reaearch work in modeling and contol of solar plants with emphasis on LFR small scale plants.

2.1. Solar field modelling

Modeling of solar field is generally carried out using longitudinal and transverse distributed model by emplying calcultion nodes in both fluid flow and transverse directions [13]. Each transverse node represents solar collector component such as the glass cover, the absorber and the fluid. The most common method is a two-node method at which the solar collector is divided into a solid part and a fluid part with individual lumped thermal capacity (distributed parameter model) [14]. This model has a significant number of parameters which are usually unknown. A simplification to the previous model can be classified into either single capacitance (one node) models, at which the solar collector is considered as a whole [15], or longitudinal distributed model (fluid flow direction) that takes into account fluid temperature nodes [16].

Most of the research works on linear focus plants have concentrated on modeling and control of PTC while studies on LFR are relatively less available [17- 20]. Simplified models of the optical and thermal behavior of the LFR plant without considering the solar field dynamics have been presented in [21, 22]. The feed water mass flow was calculated depending on the absorbed thermal power from the sun. Then the mass flow to the storage was calculated depending on the optimization of the required electrical power. A distributed parameter model was used in [22- 24] for LFR modelling. The heat loss of both metal and heat transfer process in addition to geometric efficiency were ignored. Controlled Auto-Regressive Integrated Moving Average model (CARMA) was used in [24] to identify the model parameters. Higher order controlled autoregressive (CAR) model was applied in [25] to identify the parameters using forgetting factor recursive least square method. Although, the proposed methods were used for controlling the outlet temperature of LFR, the results lacked validation of the developed models with experimental data. A detailed distributed parameter model of LFR was applied in [14, 26]. It has been concluded that the distributed parameter model was close to real data in case of clear day, while the model showed a larger error with respect to real data in the presence of wind and clouds [14]. A comparison between the experimental data of both distributed and concentrated parameter models was carried out in [26, 27] and they concluded that, the distributed parameter model is a better representative of LFR than the concentrated parameter model.

However, the distributed parameter model has a significant number of parameters which are related to geometrical and thermal properties of the fluid and materials. Using simplified models is an effective method to represent the solar collector dynamics with a minimum number of parameters that are easy to obtain via solar thermal collector standard testing. Several standard tests have been developed to normalize the solar collector's performance data.

A small-scale LFR collector was modeled using two different tests in [15]. The first one is a quasi-dynamic testing method with modifications to be compatible with the specifications of LFR collector. It was based on a one-node collector model, while the mass flow was assumed to remain near a constant value and inlet temperature was assumed to vary in a narrow range. Moreover, diffuse radiation and end loss effect were considered. Multiple Linear Regression (MLR) method was used as the parameter identification tool. The second method was a dynamic testing method based on a parameter identification and optimization of a multi-node collector model without any constraints on mass flow and inlet temperature. They concluded that the diffuse irradiation effect can be neglected for concentrating collectors with a concentration ratio larger than 80. Both methods proved to be good representatives of LFR modeling and testing. Although the quasi-dynamic testing method presented the smallest error, the dynamic testing one seemed to be better as it doesn't consider constraints on inlet data.

On the other hand, some related researches presented modelling approaches using specific libraries in widely used simulation environments such as Modelica [28, 29], TRNSYS [30,31] and Apros [32].

2.2 Solar field control

From the control point of view, as the energy source in solar plants is non-manageable, a well- developed control is essential for the fulfilment of power requirements. The solar collector plant suffers from disturbances such as variation in solar radiations, mirror reflectivity, ambient and inlet oil temperature, which cause a fast variation in the outlet temperature that must be compensated [33]. The control of the distributed solar collector plant aims to maintain the outlet temperature of the field near a desired value in spite of these disturbances. Research studies on the control of LFR soalr plants are very few in comparison to the considerable number of studies applied to control PTCs which varies between conventional and advanced control strategies. Many of of the control techniques for PTC were designed and tested on the solar parabolic-trough plant of ACUREX at the plataforma solar de Almería [33].

Concerning the control methods applied to maintain the outlet temperature of the LFR solar collector, they were inspired by different types of predictive control schemes such as generalized predictive control optimized by particle swarm (PSO-GPC) control algorithm [24], multi-model predictive switching controller [25], explicit model predictive control [26] and a feed-forward sliding mode predictive control which was presented by [23]. The applied reference set points were varying between constant and difference between inlet and outlet temperature either every sample time or holding for a period of time.

In a recent study [34], PID with suitable parallel feed forward loops has been applied to control the outlet temperature of LFR solar collector in single phase flow. The adopted model was a lumped element model that considers the absorber tube as one concentrated element. The main simplifying assumption was neglecting the temperature

distribution along the absorber tube length. The model parameters were obtained experimentally using step response reaction curve identification.

Gain scheduling model predictive control plus series feedforward controller has been applied in [35] for controlling the outlet temperature of LFR solar collector. The distributed parameter model was used for simulation purposes and the concentrated parameter model was used for obtaining a feed forward controller. In a related study [27], an incremental offset-free state-space model predictive controller has been developed for the Fresnel collector field. The controller performance was compared with the approach reported in [35] and showed better response in terms of tracking and disturbance rejection.

3. Outlines and Contribution of Present Work

The present article presents simulation and control study of a small-scale multi-generation LFR solar power plant located in SEKEM medical center near Belbis city, Egypt. Because of the nonlinear effects in the solar plants, fixed parameter PI controllers won't be able to cope with the control problem. In this article, a comprehensive study has been carried out for the use of model based feed forward control in combination with a PI controller to control the Linear Fresnel Collector plant. The main contribution of this paper and significant differences with previous reported work are summarized as follows:

- The controller is applied to a LFR small scale plant not on a parabolic trough. The plant uses oil as heat transfer fluid with thermocline stoarge tank.
- Conventional and Renewable Energy Optimization Toolbox (CARNOT) has been adopted for the first time to model the LFR solar field [36]. A quasi-dynamic distributed parameter model of LFR has been implemented in the environment of MATLAB/Simulink, which includes LFR collector, storage tank, pipes and centrifugal pump.
- The applied model is different from the models adopted in [14, 15, 27, 34, 35]. It is based on quasi-dynamic standard collector testing without constraints on inputs. The lumped parameter model mostly used in literature does not consider the delay between the collector inlet and outlet temperatures. Moreover, the model takes into account the effects of end loss, wind speed, sky temperature, cleaneness factor and tracking error [14, 16].
- Both parallel and series configurations of feed forward Proportional Integral (PI) controller with an anti-reset mechanism have been developed. The controller has been applied to maintain the difference between the outlet and inlet temperature of LFR collector at a constant value under different conditions of disturbances due to variation of ambient temperature, inlet oil temperature and solar radiation. The performance of the controllers has been thoroughly evaluated under nominal conditions, presence of disturbance, and change in operating conditions.
- The optimal controller parameters have been determined based on the integral time of absolute error (ITAE) using a function "fminsearch" from MATLAB Optimization Toolbox.

The paper is organized as follows: Section 4, briefly describes the configuration of the SEKEM plant. Section 5 describes the simulation tool. Validation of the proposed model is presented in Section 6. The different control algorithms, used to regulate the temperatures in the LFR field, are outlined in Section 7. In Section 8, the results of the numerical tests are illustrated and discussed followed by concluding remarks.

4. Plant Description

The LFR plant is installed in SEKEM medical center near Belbis city, Egypt. A scheme of the LFR plant is shown in Fig.1. It consists of LFR solar collector field, thermocline storage tank, organic Rankine cycle (ORC) and thermally driven chiller (TDC). The plant is designed to produce 120 kW thermal peak with a total collector area of 296 m^2 [37]. The solar field consists of 13 modules; one basic IFC-1832 solar collector module has approximately a total length of 4 m and 18 rows of mirrors, each 0.32 m wide. Each mirror is produced with a specific curvature in order to focus the reflected beams into the absorber tube. The heat transfer fluid, Therminol 66, is pumped through the storage system to the LFR where it gets heated up to the nominal temperature of 140-160°C. Then the heat transfer fluid is pumped from the storage system to either ORC or TDC or both using separate pumps for each component. The present article focuses on the subsystem including the LFR collector and the thermocline storage tank. The thermally driven chiller (TDC) as well as the organic Rankine cycle (ORC) will be included in the future expansion of the work.

5. Simulation of LFR Plant

In the present work, the simulation tool Matlab/Simulink using CARNOT blockset is applied for the first time for modelling LFR solar collector. The CARNOT blockset has been developed by Solar Institute Juelich for solar thermal applications and it is commercially available since 1999 [36]. It provides models for heat sources, material properties, storage systems, hydraulics and measurement elements.

The components are connected by thermo hydraulic vectors (THVs) that are containing all thermal and hydraulic information about the flow. CARNOT blockset has been previously used to model flat plate collector [38, 39]. This is the first implementation of CARNOT blockset for the simulation of the LFR solar field. Figure. 2 illustrates the

Simulink model of the SEKEM solar plant that comprises a

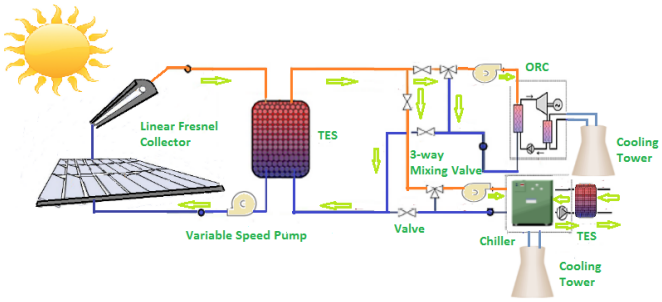

Fig.1. Schematic layout of LFR multi-generation plant.

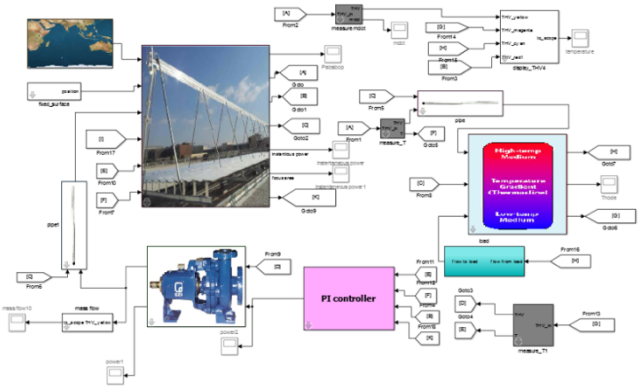

Fig.2. Simulink model of a SEKEM solar plant.

LFR as a heat source, thermocline storage tank, variable speed pump, pipes and the load.

5.1. LFR Collector Model

LFR is modeled using a one-dimensional multi-node approach. Codes are implemented in C language and linked to the simulation environment via an S-function. The LFR collector is divided into "N" nodes and the energy balance for every node is considered as:

$$C_{col}\frac{dT}{dt} = U_1(T_{amb} - T) - U_2(T_{amb} - T)^2 + U_{sky}(T_{sky} - T) + U_{wind}V_{wind}(T_{amb} - T) + \frac{\dot{m}.C}{Anet}(T_{lastnode} - T) + \eta_{opt}DNI \quad (1)$$

The three characteristic angles of horizontal LFR are shown in Fig.3[40]. The incidence angle θ_i is the angle between the sunray and its projection on the transversal plane. The other two angles are the projection of the incidence angle on the longitudinal plane $\theta_{\parallel}$ and on the transversal plane$\theta_{\perp}$. The peak optical efficiency of a collector ($\eta_{opt,0}$) is the ratio of the solar energy absorbed by the receiver to the direct normal irradiance on the aperture area [41]. This efficiency considers all optical losses of the collector for the vertical position of the sun. For adapting to the current position of the sun, the incidence angle modifiers (IAM ($\theta_{\parallel}$) and IAM ($\theta_{\perp}$)), which describe the collector losses depending on the incidence angles, are considered. IAMs are unit-less multipliers, which are characteristic of each individual collector and can be determined through standardized test procedures [42].

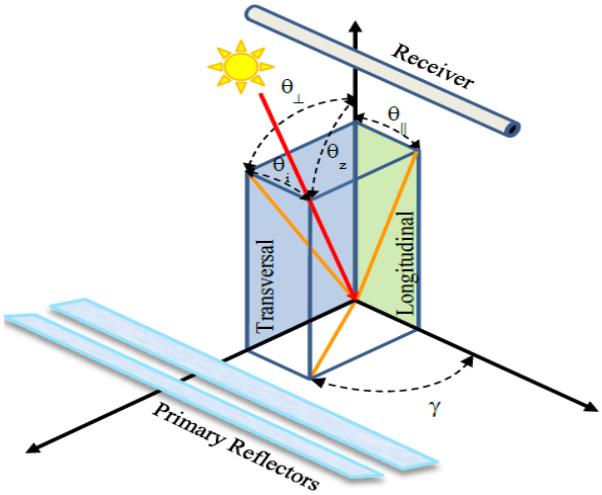

Fig.3. Characteristic angles for horizontal LFR.

These angle modifiers include cosine effect, primary reflectors mutual blocking and shading, secondary reflector and support shading, optical properties variation and intercept factor modification [42]. They can be presented either in polynomial equations form or graphs. A further reduction of the efficiency is due to end losses, i.e. to the radiation is reflected from the mirrors, but is not concentrated on the receiver due to the declination of the sun rays. The end losses efficiency factor is defined as:

$$\eta_{end\ losses} = 1 - \tan(\theta_i)\frac{x}{L_{reciever}} \quad (2)$$

Thus, the optical efficiency for the Linear Fresnel Reflector can be expressed as:

$$\eta_{opt} = \eta_{opt,0}\,.\,IAM\,(\theta_{\parallel})\;IAM\,(\theta_{\perp}).\eta_{end\ losses} \quad (3)$$

5.2. Thermocline tank model

The output thermal energy from LFR plant depends on various factors such as; ambient temperature, wind speed, solar irradiance, which varies from time to time. Thus the integration of thermal energy storage (TES) is necessary to fulfill the mismatch between thermal energy supply and energy demand [43].

The thermocline thermal energy storage applied in SEKEM plant consists of only one tank. The hot fluid is stored on the top of the tank, while the cold one is stored on the bottom because of the density difference. The intermediate temperatures between hot and cold fluid called thermocline.

The model of the storage tank is divided into several nodes. The heat flow from the collector is injected directly into the first node from the top below collector temperature. The fluid enthalpy is a result of the summation of heat-loss term, upwards and downward heat conduction, collector mass flow and load mass flow. For every node the energy balance equation (Eq. 4) is considered as [36]:

$$\rho C\frac{dT}{dt} = \frac{UA_{loss}}{V_{node}}(T_{amb} - T) + \frac{\lambda_{eff}}{\Delta z^2}(T_{node\_above} + T_{node\_below} - 2T) + \frac{\dot{m}_{coll}C}{V_{node}}(T_{node\_above} - T) + \frac{\dot{m}_{load}C}{V_{node}}(T_{node\_below} - T) \quad (4)$$

5.3. Centrifugal pump model

Operation of centrifugal pump can be described by Eq. (5) that shows the influence of flow rate on the produced pump pressure while the speed is considered to be constant.

$$\Delta P = a_0 + a_1\dot{m} + a_2\dot{m}^2 \quad (5)$$

Variable speed pump changes mass flow rate $\dot{m}$ linearly with varying speed n. To determine the approximate pump characteristics at any speed, affinity law in Eq. 6 are used [44]:

$$\frac{\dot{m}_i}{\dot{m}_j} = \frac{n_i}{n_j} \quad \& \quad \frac{\Delta p_i}{\Delta p_j} = \left(\frac{n_i}{n_j}\right)^2 \quad (6)$$

Where an index i denotes initial states and j denotes new states of the variables. For each sample time, the mass flow rate can be determined at the point in which the pump curve intersects with the system curve. Pressure drop of the system can is considered as:

$$\Delta P = b_0 + b_1\dot{m} + b_2\dot{m}^2 \quad (7)$$

5.4. Pipe model

Pipe model is considered a one-dimensional multi node model. It is a function of the heat capacity of the wall, heat losses to the environment, thermal conductivity between nodes and heat transfer by mass flow. The differential equation for each node (Eq. 8) is considered as [36]:

$$\frac{C_{wall}\,L}{V_{node}}\frac{dT}{dt} = \frac{UA_{loss}}{V_{node}}(T_{amb}-T) + \frac{\lambda_{eff}}{\Delta z^2}(T_{lastnode}-T) + \frac{\lambda_{eff}}{\Delta z^2}(T_{nextnode}-T) + \frac{\dot{m}C}{V_{node}}(T_{lastnode}-T) \quad (8)$$

5.5. Weather data

The Meteorological Data (TMY2) of Egypt are used for the development of the weather data. For the creation of the data file a specific groundwork is made to create the appropriate data file to be recognizable by CARNOT.

6. Model Validation

The validation of LFR model is carried out by comparing two sets of experimental data with the simulation results under certain operating conditions. Experimental data are obtained from LFR collector in the test field of ARCA in Palermo, Italy, at latitude 38.10044° north and longitude 13.34399° east. The data specification for the two tests of are given in Table 1.

Test 1 is performed during a period of 3 hours, while test 2 is performed during a period of 4 hours. The measured weather, flow rate and field inlet data are fed to the model. The model validation is performed by comparing the outlet temperature of the simulated and real systems without applying any type of control. The simulation results are shown in Figs. 4 and 5. Both Figures show the actual measured solar radiation intensity, input oil flow rate, the results of Simulink model against experimental results together with the inlet temperature and the corresponding error for tests 1 and 2, respectively. It can be observed that, there is a good agreement between the calculated outlet temperature of LFR model and the measured one. The maxium value of error between the measured and predicted outlet tempertaure is less than 2°C (1.2%). In view of the validation results, the capability of the presented model to predict the outlet temperature of the collector is evident and the model can be used for further analysis of the whole plant and testing different control strategies.

7. Control Strategies

Control of the solar power plant aims to maintain either the collector outlet temperature or the temperature difference over the collector field (difference between outlet and inlet fluid temperatures) near a desired value. This is manipulated by varying the oil flow pumped through the field. Here, the

Table 1. Data specification for model validation

	TEST 1	TEST 2
Date	23 of June 2017	30 of June 2017
Active modules	7	7
Area of each module	23.04 m^2	23.04 m^2
Heat transfer fluid	Paratherm NF diathermic oil	Paratherm NF diathermic oil
U_1	0.00729 $W/m^2°K$	0.00729 $W/m^2°K$
U_2	0.00043 W/m^2K^2	0.00043 W/m^2K^2
Max thermal efficiency	0.64	0.64

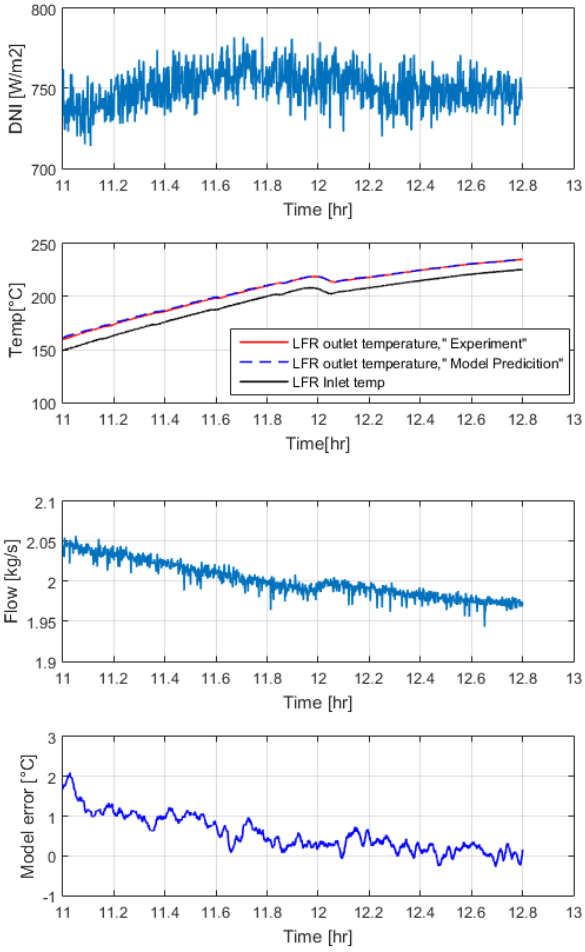

Fig.4. Comparison of model predictions with experimental measurements, test 1, refer to test conditions in Table 1.

proportional integral PI-controller is used to control the variable speed pump of LFR plant. The PI controller is developed based on its two capabilities; proportion and integration actions. The transfer function corresponding to the parallel form of the PI controller is considered as:

$$C(s)=K_p\left(1+\frac{1}{T_i s}\right) \quad (9)$$

The solar collector field suffers from disturbances such as variation in solar radiations, mirror reflectivity, ambient and inlet oil temperature, which cause a fast variation in the outlet temperature that must be compensated [33]. A feed-forward controller is a way to correct the effect caused by external and measurable disturbances, which leads to improving the performance of the closed loop system.

Feed forward controller can be used either in parallel or series configuration [33]. The block diagrams of both parallel feed forward plus the PI controller (PARFFPI) and series feed forward plus the PI controller (SERFFPI) are shown in Fig. 6.

In PARFFPI, both PI and feed-forward term calculate the oil flow rate separately then it is summed to calculate the flow q_{PAR} required to track the reference temperature and reject disturbances. In SERFFPI, the oil flow q_{SER} is calculated by the feed-forward term based on the reference temperature out from PI controller T_{ff}.

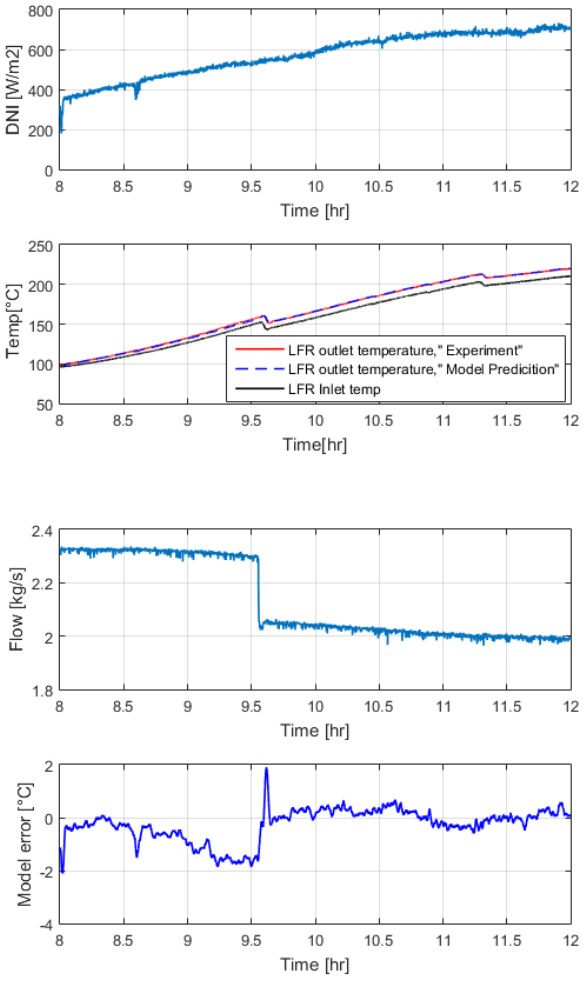

Fig.5. Comparison of model predictions with experimental measurements, test 2, refer to test conditions in Table 1.

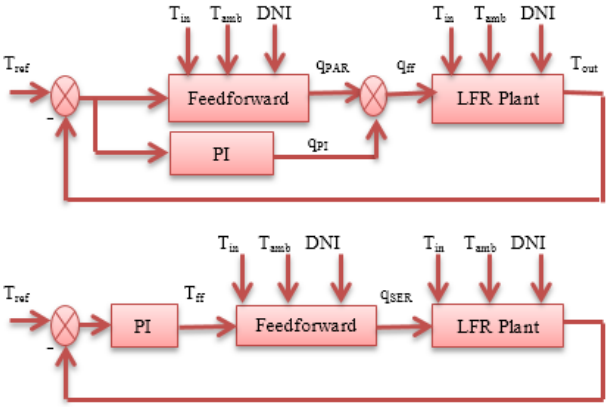

Fig. 6. PI plus Parallel feed forward scheme (top) and PI plus series feed forward scheme (bottom).

By applying the thermal balance equation (Eq. 10) of the absorber pipe:

$$\dot{Q}_{useful}=\dot{Q}_{abs}-\dot{Q}_{loss}=\dot{m}\,\Delta h$$
$$\dot{Q}_{abs}=DNI.A_{net}\,\eta_{opt}\eta_{end\ losses}$$
$$\dot{Q}_{loss}=\left[a_1\left(\frac{T_m-T_{amb}}{DNI}\right)+a_2\left(\frac{T_m-T_{amb}}{DNI}\right)^2 DNI\right]A_{net}DNI$$
$$\Delta h=C_p(T_{ref}-T_{in}) \quad (10)$$

The parallel feed forward term output q_{PAR} can be calculated as:

$$q_{PAR}=\frac{\dot{Q}_{abs}-\dot{Q}_{loss}}{Cp\,(T_{ref}-T_{in})} \quad (11)$$

The function related to the series feed forward term q_{SER} can be calculated as:

$$q_{SER}=\frac{\dot{Q}_{abs}-\dot{Q}_{loss}}{Cp\,(T_{ff}-T_{in})} \quad (12)$$

Based on the integral time of absolute error (ITAE), optimal controller parameters are determined using a function "fminsearch" from MATLAB Optimization Toolbox.

In particular, the optimum PI, PAFFPI, and SEFFPI coefficients has calculated by minimizing the objective function (Eq. 13):

$$ITAE=\int_0^t t|r(t)-y(t)|\,dt \quad (13)$$

where r is the reference temperature, y is the actual temperature and t is the simulation time. In case of saturation of the actuator, the system will be operated in an open-loop, where the control error decreases slowly and the integral term winds up [45]. The anti-windup PI controllers is responsible for canceling the integral term when the actuator is saturated, keeping the PI correction action within the saturation limits. Here, Back-calculation is used as anti- windup mechanism to cope with this situation as shown in Fig 7. It consists of re-computing the integral term in case of controller saturation as:

$$e'=\frac{1}{T_t}(u'-u)+\frac{K_p}{T_i}e \quad (14)$$

8. Numerical Simulations

This section shows the results obtained by applying PI, PARFFPI and SERFFPI controllers to control the outlet temperature of the SEKEM LFR plant. Both the set point tracking features and the disturbance rejection capabilities are tested under nominal conditions on 1st of July. Moreover, the controllers are tested against varying operating conditions used in obtaining the controllers' gains. For evaluating the

controllers' responses, their performances are analyzed using four indices [46]: integral of absolute error (IAE), integral of the square error (ISE), ITSE (integral of time-weighted square error) and ITAE.
IAE reflexes the cumulative error and does not add weight to any error. ISE gives more importance to larger errors than small errors. The error function in both ITSE and ITAE have been multiplied with time, which emphasizes long-duration errors. This makes it suitable for systems requiring a fast settling time. The smaller the values of these indices, the better the performance of the controller.

Table 2. Tuned parameters different controllers

Controller	Kp	Ti
PI	0.1719	41.9422
PAFFPI	0.1746	48.0043
SEFFPI	1.5077	129.4507

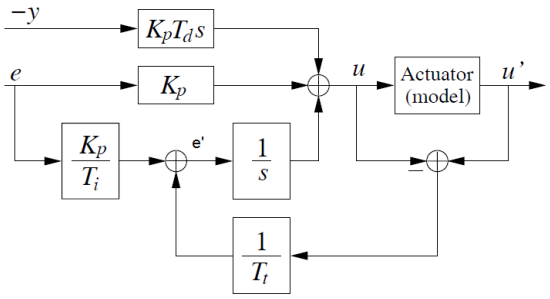

Fig.7. PID plus Anti-windup scheme with back-calculation.

The controller is used to maintain the difference between the outlet and inlet temperature at 20° C, with a time window of 30 minutes. The resulting tuned parameters of the controllers are shown in Table 2.

According to the control strategy of the SEKEM plant, Therminol oil 66 is pumped through the LFR field, where the initial temperature of the oil, when tracking starts, is close to 80 °C and it gets heated up to the nominal temperature of 140-160°C. The flow through the absorber pipe can be adjusted by a variable speed pump. The allowed fluctuation range of the flow rate of SEKEM plant is considered to be between 0.5 and 3.4 kg/s. When the oil temperature in the storage tank reaches 130°C, the flow rate of 1.9 kg/s withdraws from the tank, while the tank inlet temperature is 105°C. This procedure is done untill the outlet temperature of the storage tank decreases to 125°C.

8.1. Performance of different controllers subject to nominal conditions

A part of the test where the performance of the applied controllers can be compared has been taken from 8 AM to 2 PM. The solar radiation data of TMY2 of 1 July at the specified time are shown in Fig. 8. the flow rates are shown in Fig. 9. It can be observed that the PI controller has saturated from 12.7 PM till 14 PM, while SERFFPI and PARFFPI have saturated at 13.5 PM. For the behaviors of different controllers, as shown in Fig.10b, it can be noted that PAFFPI presents the largest overshoot at each time step with a maximum overshoot of 4.5°C. These overshoots result from adding the feed forward term to PI controller. SEARFFPI results in an over damped response at each time step as compared to an under damped response of PI. At about the noon time, 12:30 PM, all the controllers actions have saturated due to the increase of the inlet collector temperature and reaching the maximum allowable pump flow rate. From 12:30 PM till 13:30 PM, the PI controller has a significant oscillatory behavior due to variation in inlet collector temperature induced by mass flow withdrawal from the storage tank and associated response of the pump flow rate. Both PARFFPI and SEARFFPI controllers exhibit stable performance against the disturbances arise from inlet temperature variations. This represents an advantageous operating conditions for the circulation pump since the oscillatory behavior of the pump may affect its operating life. Figure 10a shows the tracking error for different controllers. From 8.5 PM till 12 PM, the maximum steady state error of PARFFPI, SEARFFPI and PI controllers are 2.8e-3 °C, 4e-3°C and .082 °C, respectively. Figure 11 shows the variation of storage tank nodes temperatures using different controllers.

Figure 12 shows the performance indices calculated for different controllers. It is clear that PI controller has the largest performance indices. The performance indices of PARFFPI

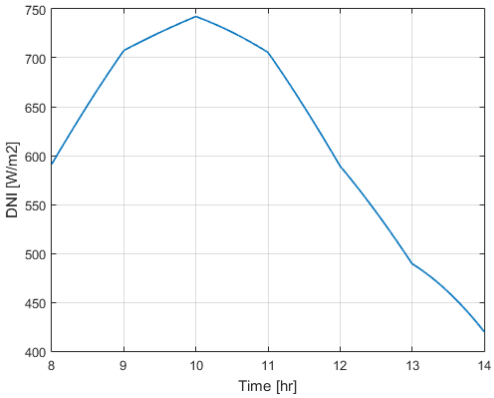

Fig. 8. Soalr radiation data on 1 July.

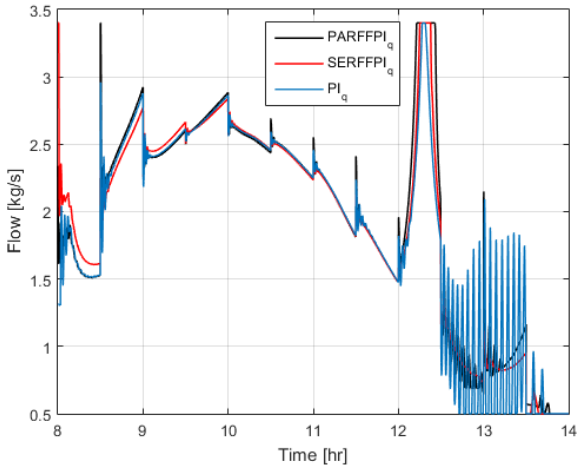

Fig. 9. Flow rates of different controllers under nominal conditions with $\Delta T = 20$°C.

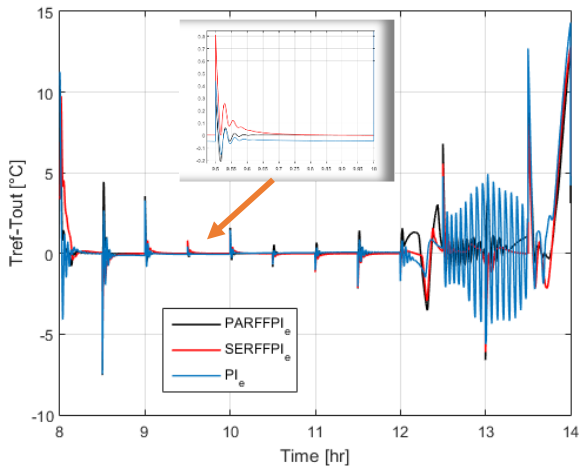

Fig. 10a. Collector's tracking error with different controllers.

and SERFFPI are close to each other. PARFFPI has the smallest performance indices of ISE and ITSE. While SERFFPI has the smallest performance indices of IAE and ITAE.

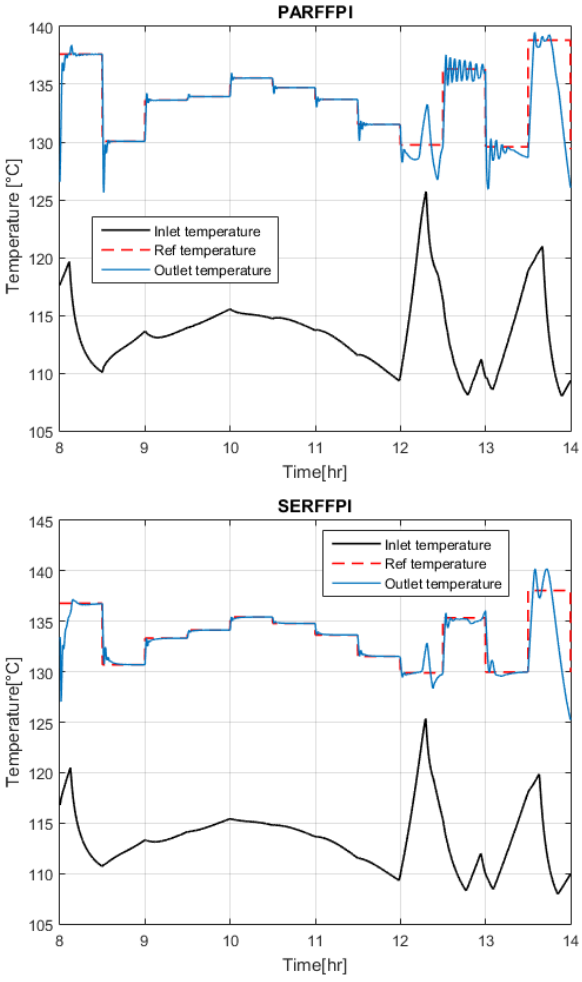

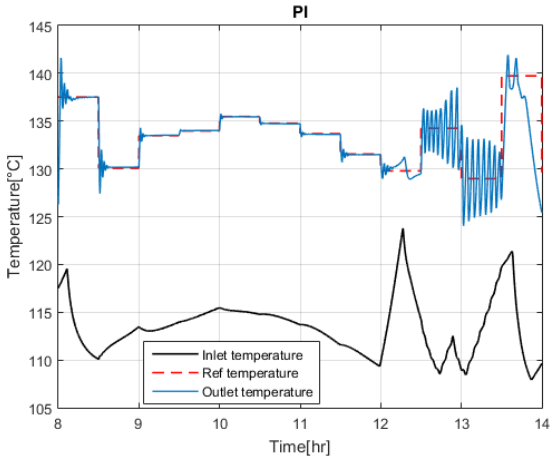

Fig. 10b. Collector's outlet temperature under nominal conditions with $\Delta T = 20℃$.

8.2. Robustness with respect to radiation disturbance

The behavior of the plant subjected to an external disturbance has been investigated. This sort of disturbance may occur when the sky is suddenly covered by clouds, that disappear after a short period of time, causing a sharp drop in the amount of radiation. An example of such disturbance is shown in Fig.13. The DNI value has suddenly dropped from

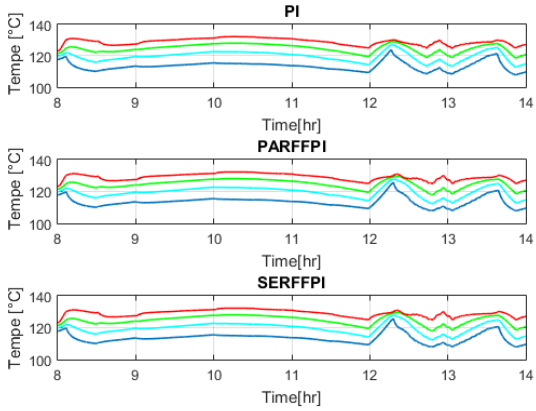

Fig. 11. Storge tank nodes temperatures of different controllers under nominal conditions with $\Delta T = 20℃$.

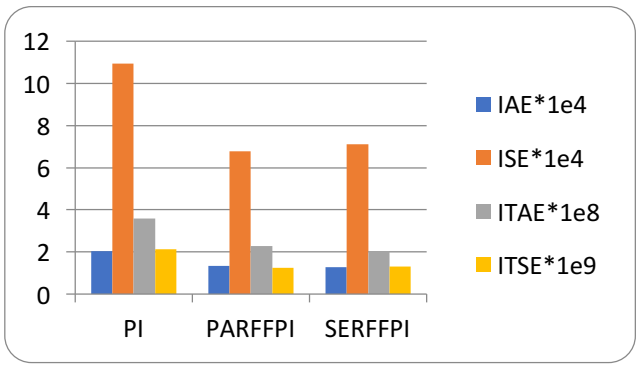

Fig. 12. Performance indices calculated to the response of different controllers in case of $\Delta T = 20℃$.

740W/m^2 to 340 W/m^2, to be back to the higher value after about 6 minutes. Fig.14 shows the different controllers' response to that disturbance. The corresponding variation of flow rate is shown in Fig.15. It can be observed that, PI controller is not adequate for rejecting radiation disturbances.

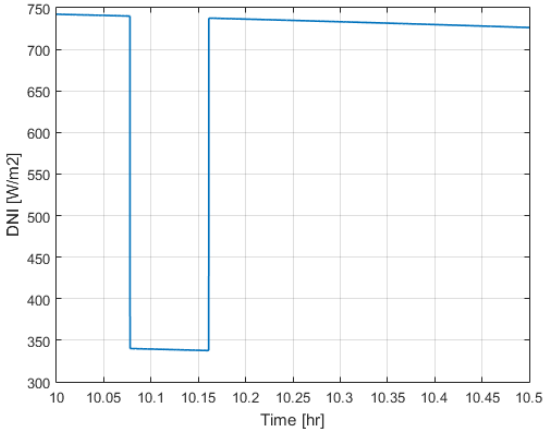

Fig. 13. Radiation data on 1 July subjected to radiation disturbance of 400 W/m^2.

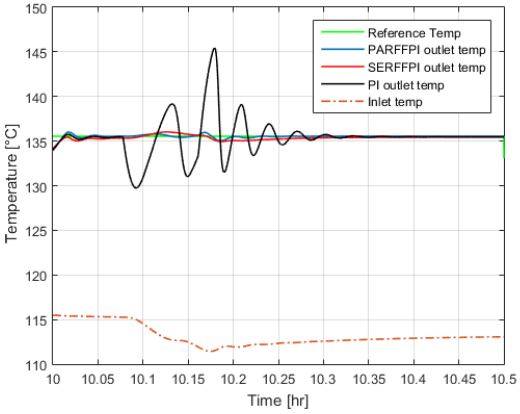

Fig. 14. Performance of different controllers subjected to radiation disturbance of 400 W/m2.

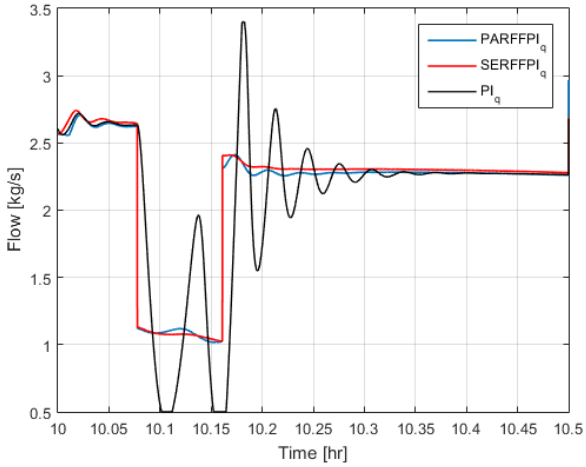

Fig. 15. Flow rates of different controllers under nominal conditions related to radiation disturbance of 400 W/m^2.

Both of PARFFPI and SERFFPI controllers show better responses for rejecting radiation disturbance. Obviously, PARFFPI is better than other controllers in dealing with this situation with a maximum overshoot of about 0.4°C as comapred to a maximum overshoot of 10 °C using PI controller. Fig. 16 shows the performance indices calculated

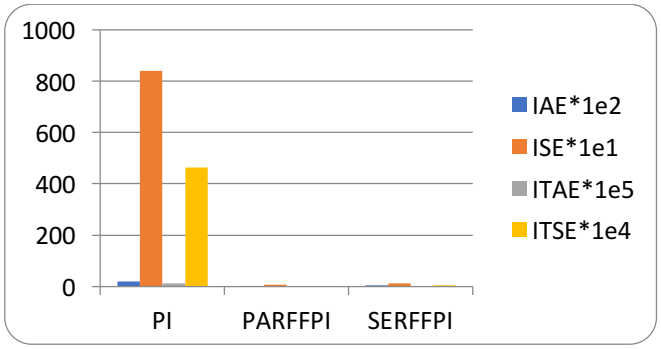

Fig. 16. Performance indices calculated as a result of radiation disturbance of 400 W/m^2.

for the different controllers related to radiation disturbance rejection. It is clear that both PARFFPI and SERFFPI have a better response in facing such a disturbance than the PI controller. However, PARFFPI is superior to SERFFPI in reducing ITSE, ITAE, ISE and IAE by 68.6%, 61.7%,41.7%, 49.1%, respectively. It can be concluded that PARFFPI is the best controller, as compared to PI and SERFFPI, for rejecting radiation disturbances.

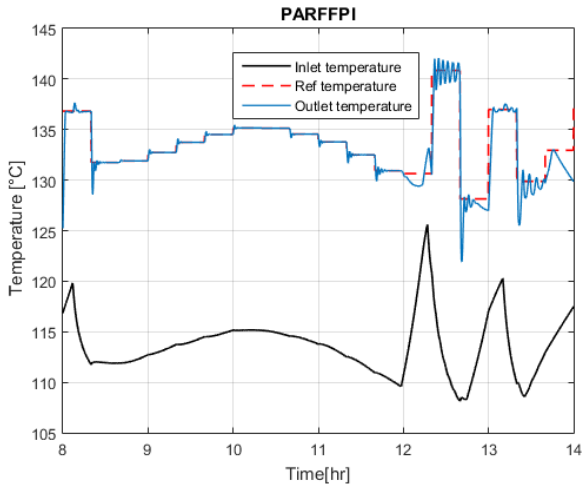

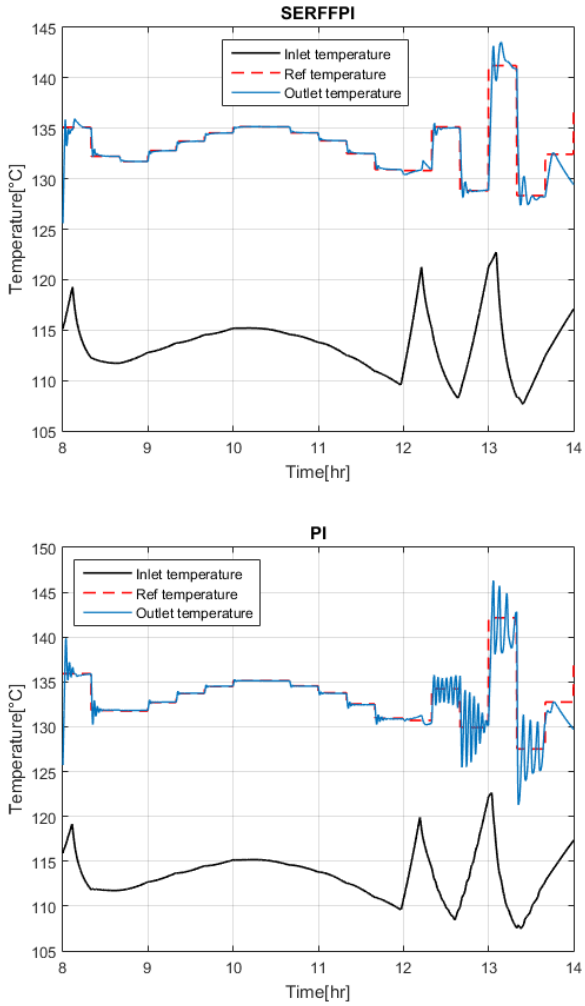

Fig. 17. Performance of different controllers as a result of changing time window to 20 minutes.

8.3. Robustness with respect to variation in operating conditions

In this section, the performance of different controllers have tested under changing in the operating conditions that used to tune it's parameters. These tests evaluate the sensitivity of controllers parametrs to changes in the operating conditions. It has been carried out with changing time window, reference temperature, and radiation data.

8.3.1. Changing time window

For checking the response of different controllers against variation in the time window (the specified time for holding the reference temperature at a constant value before changing to another value), the radiation in Fig. 8 is used, while the time window is changed to 20 minutes instead of 30 minutes. Figure 17 shows the response of different controllers to that variation. SERFFPI has presented the best performance in dealing with unexpected variation in inlet temperature. The performance indices calculated for the different controllers are shown in Fig.18. It can be observed that SERFFPI has the smallest performance indices, while PI has presented the largest performance indices. By comparing performance indices in Fig.18 to that in Fig.12, it can be seen that, the smallest time window has resulted in the smallest performance indices for all controllers. Values of IAE, ISE, ITAE, ITES for SERFFPI decreases by 42.1%, 68.12%, 43.4%, 71.5% as compared to a reduction of 28.5%, 58.1%, 33%, 66.6% using PARFFPI and 33.3%, 63.3%, 37.6% ,68.8% using PI controller. It can be concluded that SERFFPI is the most affected controller with changing the time window.

8.3.2. Changing the reference temperature

The set point is changed to 30 degrees higher than the inlet temperature of the plant with a time window of 30 minutes. Figue 19 shows the response of different controllers to that variation. Obviously, SERFFPI has presented better response than the other controllers in dealing with this situation. PI performance has declined with increasing reference temperature, it has presented a significant oscillatory behavior at the start and end of the tracking period that are not acceptable. Also, PARFFPI shows oscillatory behaviors at each time step that is not accepted for the pump operation.

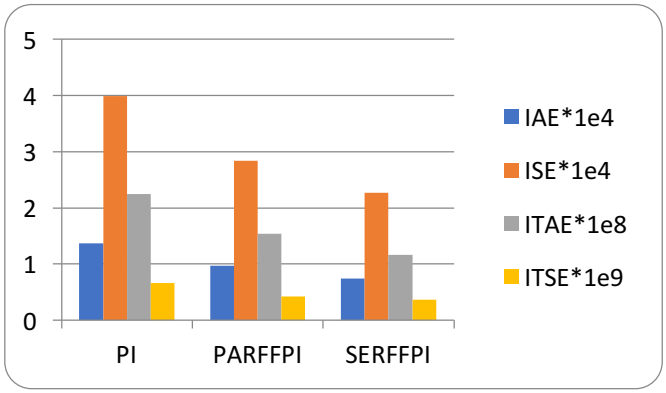

Fig. 18. Performance indices calculated for the response of different controllers as a result of changing time window to 20 minutes.

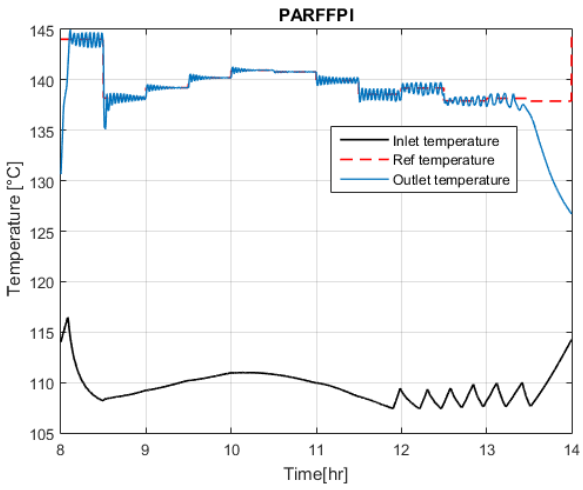

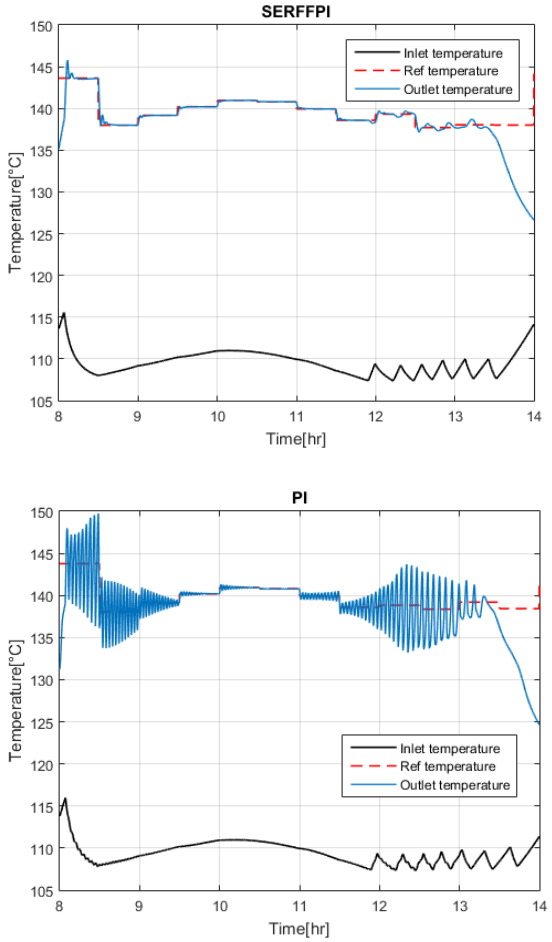

Fig. 19. Performance of different controllers with $\Delta T = 30℃$.

Figure 20 shows the performance indices calculated for the different controllers. Although performance indices of both PARFFPI and SERFFPI seem to be close, SERFFPI has presented the smallest one. On the other side, PI has presented the largest performance indices. By comparing performance indices in Fig.20 to that in Fig.12, changing the reference temperature used for tunning the controllers results in increasing the tracking errors for all controllers. Values of IAE, ISE, ITAE, ITES using SERFFPI increase by 24.7%, 39.14%, 30.2%, 40.6% as compared to an increase by 31.8%, 42.13%, 26.7%, 39.1% using PARFFPI and 49.6 %, 50.6 %, 34.2% , 39.77% using PI controller. IT is clear that, PI is the most affected controller with changing the reference temperature used for tuning the controller.

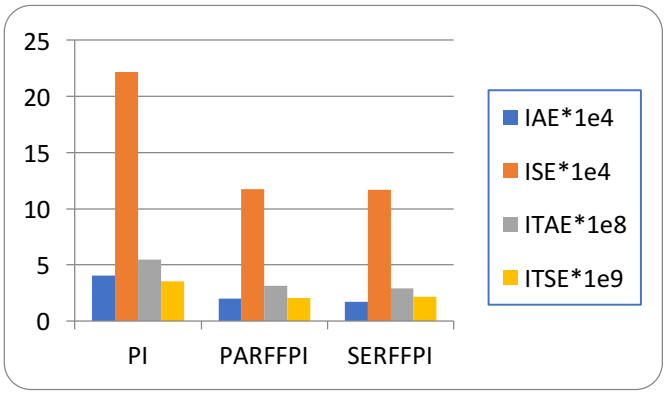

Fig. 20. Performance indices calculated to the response of different controllers with $\Delta T = 30℃$.

8.3.3. Changing the radiation data

For testing the controllers' robustness, the radiation data was taken on 21 July as shown on Fig.21. Figure 22 shows the response of different controllers on that day. Both SERFFPI and PARFFPI present better response than PI controller. From the performance indices point of view, as shown in Fig. 23, although PARFFPI and SERFFPI indices seem to be similar, PARFFPI has the smallest performance indices.

By comparing performance indices in Fig.23 to that in Fig.12, it can be seen that, changing the radiation data used for tuning the controllers results in increasing only IAE for PI by 31.08%, while ISE, ITAE, ITES decrease by 6.4%, 12.2%, 50.9% respectively. For both SERFFPI and PARFFPI controllers, IAE increases by 35.6%, 32.8% and ISE increases by 11.7%, 15.9%, respectively . On the other hand, ITAE and ITES of both SERFFPI and PARFFPI decrease by 97%, 14.3% and 49.2%, 48.7%, respectively.

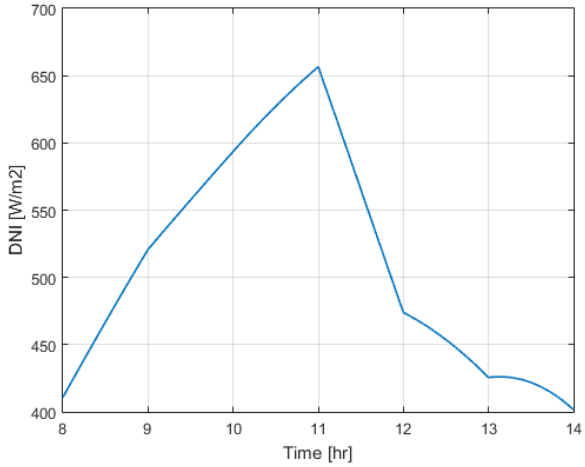

Fig. 21. Radiation data on 21 July.

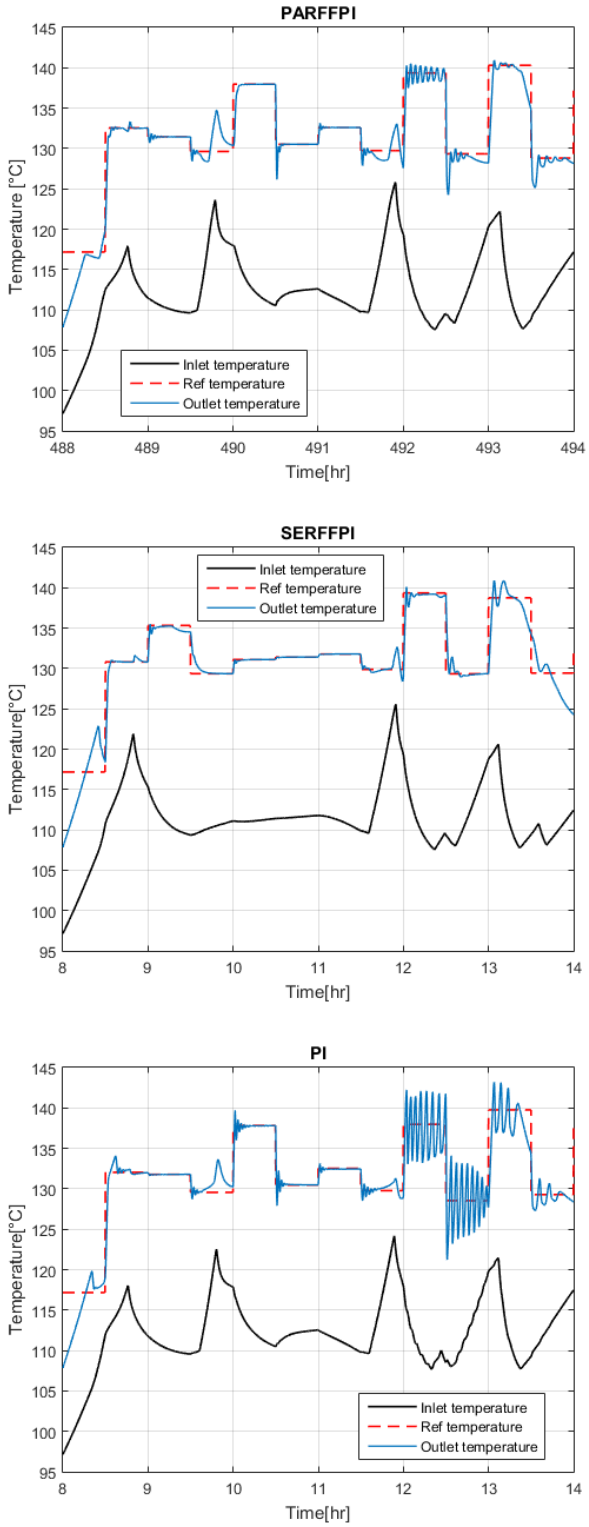

Fig. 22. Performance of different controllers on 21 July.

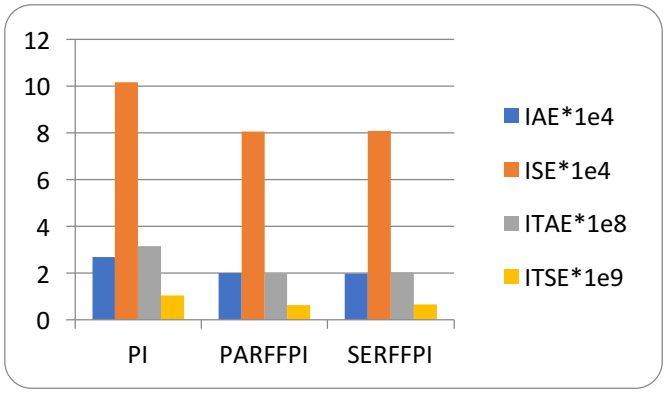

Fig. 23. Performance indices calculated to the response of different controllers on 21 July.

9. Conclusion

This paper presents a comprehensive approach for simulation and control of Linear Fresnel Reflector solar plant. A quasi-dynamic model of a LFR plant, including both the collector and the thermal storage has been implemented in the environment Matlab/Simulink using CARNOT blockset (Conventional and Renewable Energy Optimization Toolbox).

This is the first implementation of the CARNOT blockset for simulation of a LFR solar field. Validation of the developed models has been conducted by using real data extracted from an LFR plant located in Palermo, Italy. It has been shown that the results obtained using the LFR model are in good agreement with the experimental measured values.

Different control strategies based on proportional integral (PI) plus feed forward controller have been implemented to maintain the difference between the outlet and inlet temperature of the LFR collector at a constant set value. PI, PARFFPI and SERFFPI controllers plus anti-windup mechanism have been tuned using ITAE for a multigeneration LFR plant in Egypt. The controllers have been compared using four performance indices. Both feed forward controllers have shown a significant improvement against the PI controller in terms of disturbance rejection and setpoint tracking. Moreover, using feed forward controllers avoids significant oscillatory behavior in the system that may affect pump's operating life. Although SERFFPI didn't show an oscillatory behavior in tracking the setpoint, PARFFPI has proved to have a superior performance in compensating for radiation disturbance. PARFFPI is superior to SERFFPI in reduction of ITSE, ITAE, ISE and IAE for the case of radiation disturbance rejection by 68.6%, 61.7%,41.7%, 49.1% respectively. Decreasing the time window has resulted in decreasing the values of IAE, ISE, ITAE and ITES for all controllers. However, changing the reference temperature used for tuning the controllers has resulted in increasing the tracking errors and the performance indices. SERFFPI has presented the smallest values of IAE, ISE, ITAE and ITES. PI controller shows significant oscillations with the largest decrease in IAE, ISE,ITAE,ITES by 49.6 %, 50.6 %, 34.2% , 39.77%, respectively.

These observations point out the importance of applying other types of controllers to enhance the overall response for variation of operating conditions and reduce oscillations of the oil flow rate. Also, it is important to investigate both parallel and series feed forward controllers with other feedback controllers. The situation will be much more complicated when integrating the dynamics of ORC and chiller in the plant simulation model.

References

[1] H. Klaiß, R. Köhne, Joachim Nitsch, and U. Sprengel. "Solar thermal power plants for solar countries technology, economics and market potential", Applied energy, 1995.

[2] D., Mills, "Advances in solar thermal electricity technology", Solar Energy, vol 76, Issues 1–3, PP. 19-31, 2004.

[3] M. Hack, G. Zhu, T. Wendelin, "Evaluation and comparison of an adaptive method technique for improved performance of linear Fresnel secondary designs", Applied Energy, 2017.

[4] H. Evert, "The promising perspective of concentrating Solar Power (CSP)", Conference futures power system, pp. 16-18, 2005.

[5] O. Ayadi, Solar cooling systems utilizing concentrating solar collectors; design, experimental evaluation & optimization, , Ph.D. Dissertation, Politecnico di Milano, Milano, 2011.

[6] M. H. Ahmed, M. Rady, A. M. A. Amin, F. Montagnino, F. Paredes, "Comparison of thermal and optical performance of linear Fresnel and parabolic trough concentrator", 4th International Conference on Renewable Energy Research and Applications, 2015.

[7] H. Ganjehsarabi, M. Asker, A. K. Seyhan, "Energy and exergy analysis of a solar assistedcombined power and cooling cycle", 5th International Conference on Renewable Energy Research and Applications, 2016.

[8] S. Quoilin, M. Orosz , H. Hemond , V. Lemort, "Performance and design optimization of a low-cost solar organic Rankine cycle for remote power generation", Solar Energy 85, pp. 955–966, 2011.

[9] D. Lödige, B. Thomas, C. Widmann, "Intelligent management of the heat storage tank for production of electricity on demand using CHP units", 9th International Renewable Energy Storage Conference, Energy Procedia 73, pp. 239 – 243, 2015.

[10] A. Rong, R. Lahdelma, Optimal operation of combined heat and power based power systems in Liberalized power markets, 2011.

[11] G. Caua, D. Coccob, M. Petrollesec, "Optimal energy management strategy for CSP-CPV integrated power plants with energy storage", 28th international conference on efficiency, cost, optimization, simulation and environmental impact of energy systems, 2015.

[12] Montenon, F. Paredes, A. Giaconia, N. Fylaktos, S. Di Bono, C.N. Papanicolas, F.M. Montagnino. Solar multi-generation in the Mediterranean area, the experience of the STS-MED project, Eurosun 2016.

[13] S. H. López, S. L. Pérez, I. del Hoyo Arce, I. M. Dávila, "Dynamic modelling of a flat-plate solar collector for control purposes", Proceedings of the 11th International Modelica Conference September 21-23, 2015.

[14] M. Spoladore, E.F. Camacho, M.E. Valcher, "Distributed parameters dynamic model of a solar Fresnel collector field", Proceedings of the 18th World Congress, The International Federation of Automatic Control Milano, Italy, August 28 - September 2, 2011.

[15] A. Hofer, et al., "Comparison of two different (quasi-) dynamic testing methods for the performance evaluation of a linear Fresnel process heat collector", Energy Procedia 69, pp. 84 – 95, 2015.

[16] P. Isakson, "Matched flow solar collector model for TRNSYS, TRNSYS Users and Programmers Manual", 1991.

[17] M.C. Abdelkarim, T. Mohamed, C. Messaoud, and B.M. Seghir, "On the control of parabolic solar collector: the zipper approach", International Journal of Renewable Energy Research, Vol 6, No 3, 2016.

[18] R.Neves-Silva "Nonlinear control of a distributed solar field", International Conference on Renewable Energy Research and Applications, 2013.

[19] K. Noureldin, T. Hirsch, P. Kuhn, B. Nouri, Z. Yasser., R.Pitz-Paal, "Modelling an automatic controller for parabolic trough solar fields under realistic weather conditions", SolarPACES, Santiago de Chile, Chile, 2017.

[20] S. Elmetennani, I. N'Doye, K. N. Salama, T. Laleg-Kirati, "Performance analysis of fractional-order PID controller for a parabolic distributed solar collector", IEEE Africon, 2017.

[21] D. Schlipf, M. Dohn, J. Lehner, Model-based feedforward control for CSP plants with linear Fresnel technology for a flexible renewable power generation, Energy Procedia 49, pp.2191 – 2200, 2014.

[22] D. Schlipf, G. Schneider, H. Maier, "Using evolutionary algorithm to develop a feed forward control for CSP plant using mid- and long term storages", Energy Procedia 49, PP.2191 – 2200, April 2015.

[23] X.J. Lu, H.Y. Dong, "Application research of sliding mode predictive control based on feed forward compensation in solar thermal power generation heat collecting system", PP. 211–220, 2016.

[24] X.J. Lu, H..Y Dong, and D. Fan,"Particle swarm optimization applied to generalized predictive control of a solar power plant", international journal of control and Automation, Vol.9, No.2; pp.383-394, 2016.

[25] X.J. Lu, Q. GUO, H.Y. Dong, "Clustering multi-model predictive control for solar thermal power generation system", Wseas Transactions on Systems and Control, Volume 11, 2016.

[26] K.Whitheephanich, J.M. Escaño, A.J. Gallego, E.F. Camacho, "Pressurized water temperature control of a Fresnel collector field-type solar cooling system using

explicit model predictive control", 6th Asian Conference on Power and Energy Systems At: Phuket, Thailand, 2013.

[27] E.F. Camacho, A.J. Gallego, A.J. Sanchez, M. Berenguel, "Incremental state-space model predictive control of a Fresnel solar collector field", Energies, 12, 3, 2019.

[28] S. Rodat, J.V.D. Souza, S. Thebault, V. Vuillerme, N. Dupassieux, "Dynamic simulations of Fresnel solar power plants, Energy Procedia 49, pp.1501 – 1510, 2014.

[29] B. El Hefni, "Dynamic modeling of concentrated solar power plants with the ThermoSysPro library (Parabolic Trough collectors, Fresnel reflector and Solar-Hybrid) ", Energy Procedia 49, pp. 1127 – 1137, 2014.

[30] T. Sultana, G.L. Morrison, R. Taylor, G. Rosengarten, "TRNSYS modeling of a linear Fresnel concentrating collector for solar cooling and hot water applications", Journal of Solar Energy Engineering, Vol. 137, April 2015.

[31] M.H. Ahmed, A. Giaconia, A.M.A. Amin, "Effect of solar collector type on the absorption system performance", 5th International Conference on Renewable Energy Research and Applications, 2016.

[32] E. Hakkarainen, M. Tähtinen, H. Mikkonen, "Dynamic model development of linear Fresnel solar field", 9th International Conference on Energy Sustainability ES2015, June 28-July 2, 2015.

[33] E. F.Camacho, M. Berenguel, F. R. Rubio, D. Martìnez, Advances in Industrial Control: Control of Solar Energy Systems, Springer, 2012.

[34] M.M. Mokhtar, Control of solar thermal linear Fresnel collector plants in single phase and direct steam generation modes, Ph.D. Dissertation, Institut fur Neutronenphysik und Reaktortechnik (INR) , Germany, 2019.

[35] A.J. Gallego, G. Monguio, M. Berenguel, E.F. Camacho, "Gain-scheduling model predictive control of a Fresnel collector field", Control Eng. Pract, 82, 1–13, 2019.

[36] B. Hafner, J. Plettner, C. Wemhöner, "CARNOT blockset: conventional and renewable energy systems optimization blockset – user's guide", Solar-Institut Jülich, Aachen University of Applied Sciences, 1999.

[37] M.Rady, A. Amin, M. Ahmed, "Conceptual design of a small scale multi-generation concentrated solar plant for a medical center in Egypt", Energy Procedia 83:2, pp. 89–98, 2015.

[38] G.Gavriilidis, Development of a hybrid system of solar collectors and a biomass furnace, with the use of the program C.A.R.N.O.T. for covering the needs in hot water of a hotel in Greece, MSc. Dissertation, Aachen University of applied Science, Jülich, 2015.

[39] C. Trinkl, "A domestic solar/heat pump heating system incorporating latent and stratified thermal storage", 2006.

[40] A. Giostri, Transient effects in linear concentrating solar thermal power plant, Ph.D. Dissertation, Politecnico di Milano, Milano, 2013.

[41] M. Eck, et al., "Guidelines for CSP yield analysis optical losses of line focusing systems; definitions, sensitivity analysis and modeling approaches", Energy Procedia 49, pp. 1318 – 1327, 2014.

[42] T. Osório, M. J. Carvalho, "Testing of solar thermal collectors under transient conditions", Energy Procedia 30, pp. 1344 – 1353, 2012.

[43] B. Dollinger, K. Dietrich, "Storage systems for integrating wind and solar energy in Spain", International Conference on Renewable Energy Research and Applications, 2013.

[44] L. Gevorkov, Simulation and experimental study on energy management of circulating centrifugal pumping plants with variable speed drives, Ph.D. Dissertation, Tallinn university of technology, Estonia 2017.

[45] A. Visioli, "Practical PID control", Springer-Verlag London, 2006.

[46] M.A. Duarte-Mermoud, R.A. Prieto, "Performance index for quality response of dynamical systems", ISA Transactions 43, pp. 133–151, 2004.